

THE SYNTHESIS AND TURNOVER OF RAT LIVER PEROXISOMES

IV. Biochemical Pathway of Catalase Synthesis

PAUL B. LAZAROW and CHRISTIAN DE DUVE

From The Rockefeller University, New York 10021. Dr. Lazarow's present address is Department of Biological Sciences, Stanford University, Stanford, California 94305.

ABSTRACT

Early events in the biosynthesis of liver catalase were studied on female rats receiving [³H]leucine or [³H]δ-aminolevulinic acid or a mixture of [³H]leucine with [¹⁴C]δ-aminolevulinic acid by intraportal injection. Catalase antigen was selectively separated from homogenates by immunoprecipitation, both without and after partial purification of the enzyme. Label from both precursors appeared first in immunoprecipitable material which was lost upon purification of catalase; the label subsequently became associated with material indistinguishable from catalase. Kinetic analysis of the results indicates that the nonpurifiable material identified by early labeling consists of two distinct biosynthetic intermediates, the first lacking heme and representing about 1.6% of the total catalase content or 13 μg/g liver, the second containing heme and representing about 0.5% of the total catalase content or 4 μg/g liver. The first intermediate migrates at the same rate as catalase upon sodium dodecyl sulfate-polyacrylamide gel electrophoresis, and therefore has a monomeric molecular weight of about 60,000.

INTRODUCTION

It is widely assumed that peroxisomes arise in rat liver in the form of projections budding off from the endoplasmic reticulum. Experiments designed to explore some of the biochemical implications of this model have, however, failed so far to provide any support for it (17, 18). The model has not been entirely ruled out, but its possible time scale has been considerably restricted. According to available results, if peroxisomes do grow as buds off the endoplasmic reticulum, then they must reach their final size in considerably less than 3 h, and probably in even less than 1 h or 2% of their average life-span. An alternative possibility is that the peroxisomes do not exist as independent individuals in the intact cells, but are interconnected,

either permanently or intermittently, in such a way as to continually interchange their contents.

In the present studies, we have looked at the early events whereby rat liver catalase is synthesized and deposited within peroxisomes. We used radioactive tracers to label catalase, immunochemical methods to separate catalase from other liver proteins, and density gradient centrifugation to fractionate the cells. In this paper we report on the kinetics of catalase biosynthesis, which takes place by way of at least two distinct biosynthetic intermediates. In the subsequent paper we describe the cell fractionation experiments, which show the intracellular pathway followed by the intermediates (10). The results presented here form part of

the Ph.D. thesis of one of us (Lazarow [8]) and have been reported in preliminary communications (7, 9).

MATERIALS AND METHODS

Materials

Rats were obtained from Charles River Breeding Laboratories, Inc. (Wilmington, Mass.).

Labeled compounds were purchased from Schwarz/Mann (Orangeburg, N. Y.) in 0.01 N HCl. They were neutralized and adjusted to isotonicity by the addition of 0.1 vol of 0.55 M NaHCO₃ in 1.14 M NaCl.

All chemicals were of reagent grade. Bovine serum albumin (BSA)¹ was obtained as bovine plasma fraction V from Armour Pharmaceutical Co. (Kankakee, Ill.). Horse heart cytochrome *c*, bovine pancreatic trypsin, chicken ovalbumin, and bovine liver catalase were purchased from Sigma Chemical Co. (St. Louis, Mo.).

Biochemical Assays

Catalase activity was determined by the method of Baudhuin et al. (2). One unit of activity decreases the H₂O₂ concentration 10-fold per minute in a reaction volume of 50 ml at 0°C. Protein was measured by the automated Lowry technique of Leighton et al. (11), and is expressed in milligrams based on a BSA standard.

Radioactivity Determinations

Total proteins were precipitated with cold 10% trichloroacetic acid (TCA) containing 1 mM leucine and 0.5 mM δ -aminolevulinic acid (ALA). The precipitates were collected by centrifugation and washed 3 times with cold 5% TCA, containing 1 mM leucine and 0.5 mM ALA. Catalase antigen was recovered by immunoprecipitation, as described below. The precipitated proteins were dissolved in 0.1 N NaOH and a 0.5 ml sample was mixed with 10 ml of Triton-toluene scintillation fluid (9) followed by 10 μ l of glacial acetic acid. Radioactivity was determined in a Packard no. 3375 scintillation counter equipped with no. 7400056 bialkali phototubes

¹ *Abbreviations used in this paper:* ALA, δ -aminolevulinic acid; BSA, bovine serum albumin; DAB, 3,3'-diaminobenzidine; ML, mitochondrial plus light mitochondrial fraction (2); PBS, phosphate-buffered saline, 0.15 M NaCl + 10 mM phosphate buffer, pH 7.0; PBSLA, PBS containing 0.1 mM L-leucine and 0.01 mM ALA; PCI, purified catalase immunoprecipitate; SDS, sodium dodecyl sulfate; TCA, trichloroacetic acid; WLI, whole liver immunoprecipitate.

(Packard Instrument Co., Inc., Downers Grove, Ill.), at 37 and 60% counting efficiencies for tritium and carbon-14, respectively, as optimized for double-label counting.

Immunological Assays

The titer and specificity of anticatalase preparations were assessed by conventional quantitative immunoprecipitation and Ouchterlony double diffusion (using immunodiffusion cells containing reservoirs of antigens and antibody, Cordis Laboratories, Miami, Fla.), and by a semiquantitative microimmunodiffusion assay which was developed to monitor the purification of anticatalase.

Purification of Catalase

The anticatalase preparations used in previous work contained antibodies against liver constituents other than catalase, making it necessary to partly purify catalase before immunoprecipitation (17). We wished to eliminate this requirement and set out to improve the purification of rat liver catalase (12). Substituting purified peroxisomes (11) for the crude mitochondrial plus light mitochondrial (ML) fraction used previously as starting material raised the specific activity of the purified enzyme by 15% (Table I). The material isolated in this manner behaved as a homogeneous protein of molecular weight about 240,000 on Sephadex G-200 chromatography and migrated in the form of homogeneous subunits of molecular weight 60,000 on sodium dodecyl sulfate-(SDS)-polyacrylamide gel electrophoresis, indicating that only contaminants having the same molecular size and tetrameric structure as catalase could have been present in significant quantities. As will be shown below, such contaminants, if present, did not induce the formation of detectable amounts of antibodies. Despite these evidences of purity, our new preparations attain only 80% of the specific activity of those described by Price et al. (19). Possible reasons for this discrepancy have been discussed before (12).

Preparation of Anticatalase

The purified catalase was used for the purification of anticatalase from an impure rabbit antiserum, and for the production of a monospecific goat antiserum.

The anticatalase was purified by the following modification of the solid-phase immunoabsorbent technique of Avrameas and Ternynck (1): 300 mg of BSA were first polymerized by means of 0.7% glutaraldehyde in 0.2 M acetate buffer, pH 5.0. The resulting gel was homogenized into small pieces and washed. Then 4.8 mg of purified rat liver catalase were attached to the BSA gel by means of 0.2% glutaraldehyde. The gel was washed once and treated

TABLE I
Properties of Purified Catalase

Catalase preparation	Specific activity*	Activity extinction coefficient†		Mass extinction coefficients‡			$\frac{\epsilon_{407}}{\epsilon_{276}}$
		407 nm	407 nm	312 nm	276 nm	252 nm	
	U/mg						
Purified from ML fraction							
Exp. 1	52	0.031	1.58	0.30	1.47	0.96	1.08
Exp. 2	51	0.032	1.64	0.32	1.46	0.90	1.12
Purified from peroxisomes							
Exp. 1	58	0.032	1.88	0.34	1.67	1.10	1.13
Exp. 2	60	0.031	1.86	0.36	1.83	—	1.02
Calculated from the data of Price et al. (19)	73	0.023	1.68	0.29	1.55	1.04	1.085

* Equal to 10^{-3} *Kat.f.*

† Absorbance per centimeter of a solution containing 1 U of catalase activity/ml.

‡ Absorbance per centimeter of a solution containing 1 mg protein/ml (ϵ).

with several changes of 100 mM ethanolamine to block free glutaraldehyde ends. All the above operations were carried out in 0.2 M acetate buffer, pH 5.0. Finally the gel was thoroughly washed with, and re-suspended in, 0.15 M NaCl buffered to pH 7 with 10 mM phosphate (PBS). To this suspension were added 20 ml of rabbit antiserum, containing an amount of anticalase (about 13 mg, see below) approximately equivalent to the catalase on the gel, in 1.4 g of total protein. The gel was thoroughly washed with PBS and about 50% of the anticalase and more than 1.3 g of protein appeared in the washes. Therefore, the gel-bound catalase retained about 1.4 times its weight of anticalase, a value which compares favorably with the ratios of 0.2–1.0 reported by Avrameas and Ternynck (1). Anticalase was eluted from the gel with several changes of 0.1 M glycine-HCl buffer pH 2.8. The eluates were passed through a 0.22 μ m Millipore filter, and dialyzed against PBS. About 80% of the adsorbed anticalase was recovered in this manner. The gel was reused twice after thorough rinsing in PBS; there was some loss in anticalase binding capacity with repeated use.

The three batches of purified anticalase were pooled and characterized by quantitative immunoprecipitation and by immunodiffusion. As shown in Fig. 1, 300 μ l of purified anticalase are equivalent to about 0.9 U (15 μ g) of catalase. In the equivalence zone, the precipitate contains about 58 μ g of protein, which corresponds to a molar ratio of γ -globulin to catalase of 4.4 (assuming a molecular weight of 150,000 for the rabbit γ -globulins). This is a reasonable value for a protein of the size of catalase (6). The 300 μ l of

purified anticalase contained 118 μ g of protein. Of this, a maximum of 43 μ g precipitated, indicating that the anticalase was 36% pure, and therefore had been purified about 40-fold over the original serum. Immunodiffusion revealed no antibody other than anticalase in the purified preparation. The antibody solution was sterilized by filtration through a 0.22 μ m Millipore membrane and stored in the cold room. Its potency remained unchanged for at least 6 mo.

The second antibody preparation was raised in a goat with 7 mg of pure catalase. The animal was bled 2 mo after immunization, and a number of times thereafter. Globulins were precipitated from the serum by half saturated $(\text{NH}_4)_2\text{SO}_4$, washed, resuspended in an amount of 0.15 M NaCl equal to half the original volume of serum, dialyzed extensively against 0.15 M NaCl, sterilized by Millipore filtration, and frozen in small lots. Control globulins were similarly prepared from serum obtained from the goat before immunization.

The anticalase titer in the globulin preparation, determined by quantitative immunoprecipitation, was 1.2 ml of globulins (2.4 ml of serum) equivalent to 60 U of catalase. This is twice as much anticalase per milliliter of serum as we obtained in rabbits, despite the fact that the rabbits received about 10 times more antigen per unit body weight than did the goat.

The specificity of the goat antiserum was determined by immunodiffusion against purified catalase and rat liver postnuclear supernate (Fig. 2). The relative concentrations of the reactants were varied more than 100-fold (ranging from great antibody excess to

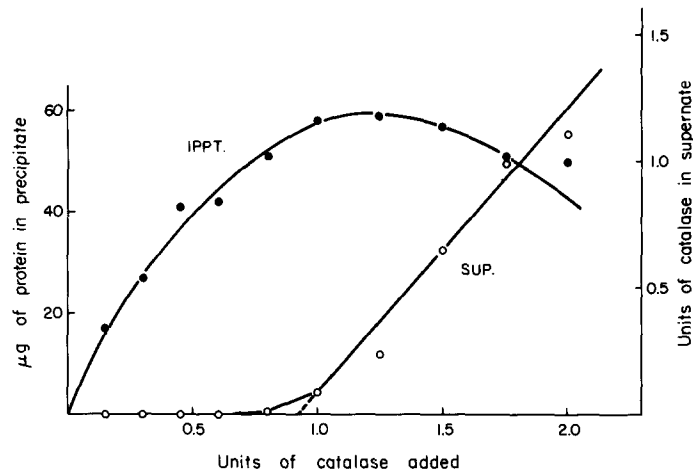


FIGURE 1 Quantitative immunoprecipitation with purified rabbit anticatalase. 300 μ l of anticatalase were incubated with various amounts of purified rat liver catalase for 1 h at 37°C and 36 h at 0°C. The immunoprecipitates (IPPT.) were washed twice and dissolved in 0.1 N NaOH for protein determination (●). Control tubes lacking anticatalase contained negligible precipitated protein. Control tubes with anticatalase alone had 4 μ g of precipitated proteins; this was subtracted from the protein determined in the immunoprecipitates. The catalase remaining in the supernate after immunoprecipitation (SUP.) was also measured (○).

great antigen excess) without revealing any immunoprecipitate other than that formed by catalase and anticatalase. This precipitate caused the evolution of O₂ bubbles when flooded with H₂O₂, and stained with the 3,3'-diaminobenzidine (DAB) reaction of Graham and Karnovsky (3) as modified by Novikoff and Goldfischer (15). When the anticatalase was replaced by control goat globulins, no immunoprecipitate could be detected. Immunoelectrophoresis also failed to reveal any contaminating antibody-antigen system.

Immunoprecipitation of Catalase

The immunoprecipitation technique used in earlier work was adapted to the separation of labeled catalase from crude liver fractions solubilized by 1% Triton X-100. Serious difficulties were encountered due to nonspecific precipitation, especially with certain mitochondrial fractions. The main factor responsible for this phenomenon was found to be protein denaturation during the 1 h incubation at 37°C. We were able to avoid this artifact to some extent by adding soluble proteins (4 mg/ml rabbit serum globulins) to the system, and more effectively by performing the immunoprecipitation entirely at 0°C, as recommended by Higashi and Kudo (5). Adsorption to glass was another source of nonspecific contamination, which was prevented by siliconizing the tubes. On the other hand, contrary to the experience of some other workers, adsorption to the immunoprecipitate itself was of minor importance in our work, and a preliminary immunoprecipitation of an added antigen (ovalbumin) did not significantly reduce contamination.

As a result of these and other trials, the following procedure was finally adopted. Frozen homogenates or subcellular fractions were thawed and treated with Triton X-100 to a final concentration of 1%. They were then diluted with an appropriate solute mixture to the following final concentrations (PBSLA): NaCl, 0.15 M; potassium phosphate buffer, pH 7.0, 10 mM; L-leucine, 0.1 mM; ALA, 0.01 mM; sucrose, <0.4 M; Triton X-100, <0.4%; and catalase, <0.8 U/ml. The samples were passed under positive pressure through 0.22 μ m Millipore filters. Catalase activity and radioactive proteins were quantitatively recovered in the filtrates. 2.5 ml of the filtered solutions were pipetted into tared, siliconized, conical, 5-ml glass centrifuge tubes, and incubated overnight at 0°C with an amount of anticatalase equivalent to 2.5 U of catalase. A second 2.5 ml aliquot was treated identically, but with control globulins. The precipitates were collected by centrifugation for 1 h at 2,000 rpm in swing-out buckets in a refrigerated International centrifuge (International Scientific Instruments Inc., Palo Alto, Calif.), washed twice with 2.5 ml of PBSLA, and dissolved by addition of 0.5 ml of 0.1 N NaOH. The tubes were weighed to provide a measurement of the total volume of the resulting solution, and a 0.5 ml sample was taken for scintillation counting. The radioactivity found in the control tubes was subtracted from that recovered with anticatalase. This correction varied between 5 and 35%, depending on the precursor and the labeling time. As a check of the overall reliability of the procedure, catalase activity was assayed systematically in the original samples and in the supernates from the im-

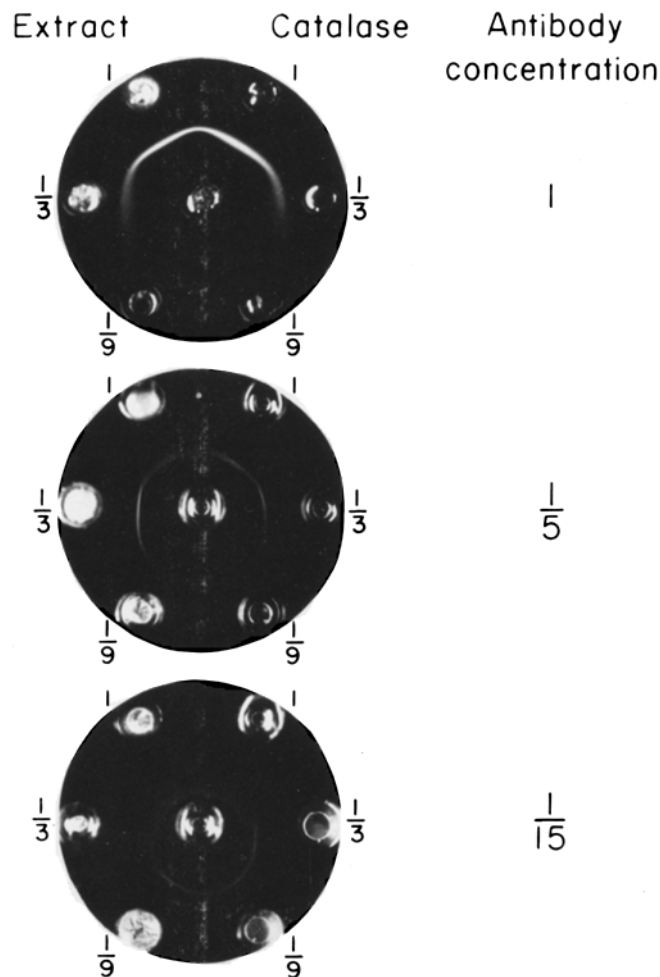


FIGURE 2 Immunodiffusion of goat anticatalase vs. rat liver extract (postnuclear supernate) and purified catalase. The undiluted extract contains 0.2 g liver/ml, the undiluted catalase contains 11 U/ml, and the undiluted anticatalase is the goat globulin preparation described in the text. Immunodiffusion was for 6 days at 0°C. The unstained precipitates were photographed by scattered light (23).

munoprecipitations. In all cases, less than 1% of the activity remained in the supernate after immunoprecipitation, as compared with 80–100% in the control supernates. Therefore the immunoprecipitations were essentially complete. Anticatalase has little effect on the activity of the enzyme, and when immunoprecipitation is not complete, catalase activity is found in the supernate (Fig. 1, open circles).

Micropurification and Immunoprecipitation of Catalase

Immunoprecipitation was carried out also after a preliminary purification of catalase, which was performed as follows: At 0°C, a 1.5 ml sample was shaken vigorously with 7 ml of 27% ethanol in 54 mM ace-

tate buffer, pH 4.1, and 0.5 ml of chloroform. After centrifugation for 1 min at 1,500 rpm, the lower chloroform phase was removed with a Pasteur pipette, 0.1 ml of 0.5 M Na₂SO₄ was added and the tube was shaken again. The resulting precipitate was collected by centrifugation for 15 min at 40,000 rpm, extracted overnight with 2 ml of 10 mM potassium phosphate buffer, pH 7.0, and recentrifuged for 30 min at 40,000 rpm. The supernate contained 50–70% of the catalase activity with 3–4% of the total protein and 5–15% of the total TCA-precipitable radioactivity (after leucine labeling). It was used for immunoprecipitation as described above, except that the Millipore filtration step was omitted. The radioactivity measured in the immunoprecipitate was corrected for the observed loss in catalase enzymatic activity upon purification.

In Vivo-Labeling Experiments

In the single-labeling experiments, 0.5–1.0 mCi L-[4,5-³H]leucine (6–15 Ci/mmol) or 2.5 mCi [2,3-³H]δ-ALA (22 Ci/mmol), in 0.5–1.0 ml isotonic solution, was injected into the portal vein of 220–260 g female Sprague-Dawley rats under Nembutal anesthesia (40 mg/kg). In the double-labeling experiments, 1.5–5 mCi [³H]leucine (6 Ci/mmol) and 0.1–0.5 mCi [¹⁴C]ALA (46.5 mCi/mmol) were given together by the same route. The animals were sacrificed after various lengths of time and their livers ho-

mogenized in 0.25 M sucrose containing 0.1% ethanol (to protect the catalase activity). The homogenates were assayed for catalase and protein, and for TCA-precipitable and immunoprecipitable radioactivities, as described above. In all cases, immunoprecipitates were separated without, as well as after, partial purification of catalase. The former, termed *whole liver immunoprecipitate* (WLI), contained all the material that was recognized by anticatalase antibodies (including at least 99% of the catalase enzymatic activity). The latter, designated *purified catalase immunoprecipitate* (PCI), contained only catalase antigen that

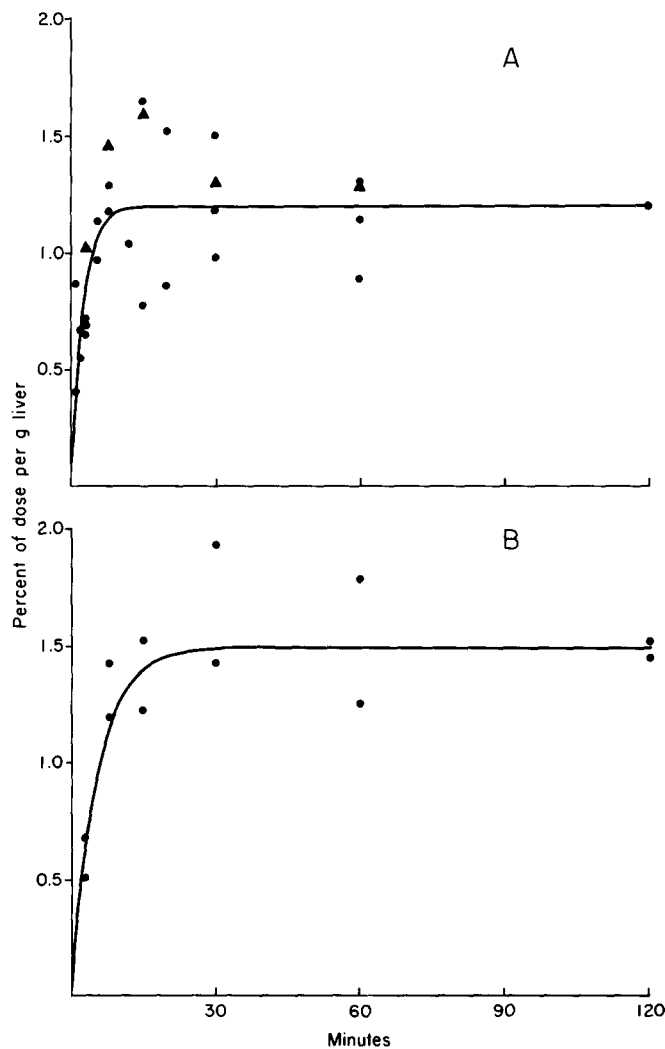


FIGURE 3 Incorporation of [³H]leucine (A) and [³H]ALA (B) into TCA-precipitable material. Circles are from single-, triangles from double-labeling experiments. Curves drawn are functions of general form: $y = y_{\max}(1 - e^{-t/T})$, with T (T_L) = 2.5 min for leucine, and $T = 5.5$ min for ALA (see Discussion).

survived purification. As mentioned, its radioactivity was corrected for the loss of catalase enzymatic activity.

RESULTS

Single-Labeling Experiments

Fig. 3 illustrates the manner in which label from either [^3H]leucine or [^3H]ALA entered TCA-insoluble material. Noteworthy is the rapid attainment of a plateau with each of the precursors. The plateau values amount to about 1.2 and 1.5% of the injected dose per gram liver, for leucine and ALA, respectively.

As shown in Fig. 4 (solid circles), incorporation of leucine into the WLI paralleled closely its incorporation into TCA-insoluble material. The plateau value is of the order of 0.0055% of the injected dose per gram liver, or 0.45% of the amount incorporated into TCA-precipitable material. The appearance of labeled leucine in the PCI followed a very different course (Fig. 4, open circles). There is a suggestion of a lag of 2–3 min, followed by a slow and gradual increase, up to a value which at the end of 2 h reaches 80% of that found in the WLI.

With [^3H]ALA as precursor (Fig. 5, solid circles) incorporation of label into the WLI occurred much more slowly than it did into TCA-insoluble material, being far from completed even after 2

h. The uptake of label into the PCI (Fig. 5, open circles) was even slower, so that a distinct difference between the radioactivities of the two immunoprecipitates, qualitatively similar to that recorded after injection of [^3H]leucine, was observed. Except for a single value, at 120 min, the proportion of total immunoprecipitable label recovered in the PCI was always larger with ALA than with leucine as precursor (Table II).

Later time points were investigated on unanesthetized animals receiving the labeled precursors by intraperitoneal injection. As shown in Table III, after 3 h the PCI contained only 70–80% of the radioactivities present in the WLI. By 18 h the difference had completely disappeared.

Fig. 6 shows the result of an SDS-gel electrophoretic analysis performed on the material recovered in the WLI 8 min after intraportal injection of [^3H]leucine. The larger part of the label migrated essentially like catalase itself. The balance presumably corresponds to the 29% of nonspecific label found in the control tube.

Double-Labeling Experiments

In the fractionation experiments reported in the following paper (10) [^3H]leucine and [^{14}C]ALA were injected simultaneously, at dosages commensurate with the requirement for measurable radioactivities in the subcellular fractions. These

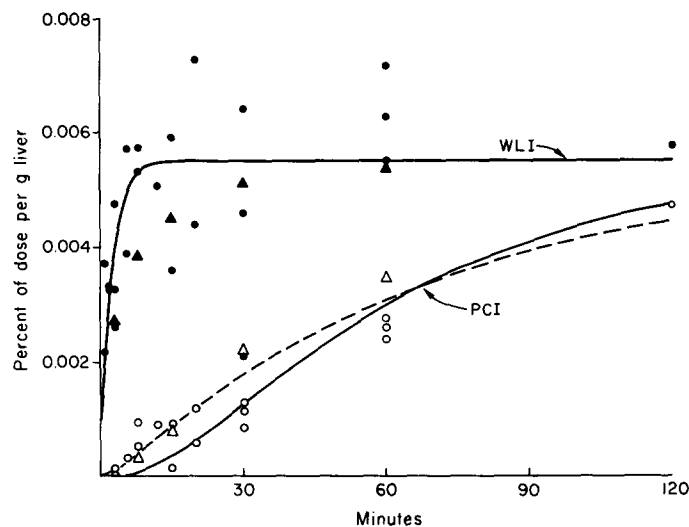


FIGURE 4 Incorporation of [^3H]leucine into WLI and into PCI. Circles are from single-, triangles from double-labeling experiments. The curve for WLI represents Eq. 12 (see Discussion) with $T_L = 2.5$ min and $L_1 = 0.0055\%$ dose/g liver. The solid curve for PCI represents Eq. 11 with $T_I = 49$ min and $T_Q = 17$ min. The dotted curve is theoretical for a one intermediate model with $T_Q = 70$ min.

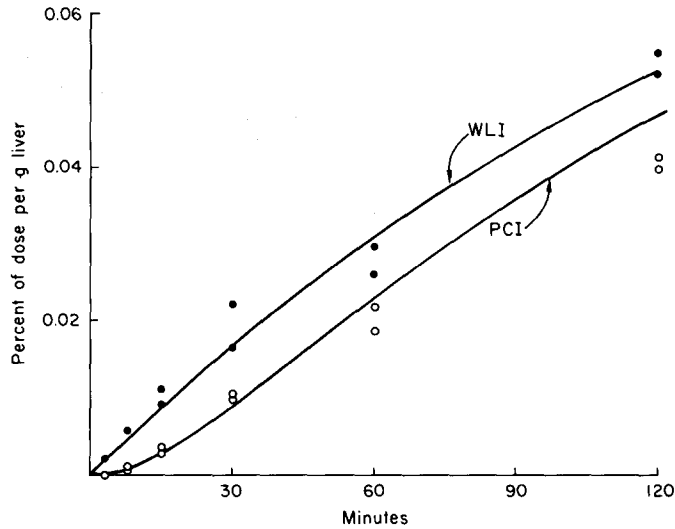


FIGURE 5 Incorporation of [^3H]ALA into WLI and into PCI. The curve for WLI represents Eq. 16 (see Discussion) with $T_H = 170$ min and $H_1 = 0.104\%$ dose/g liver. The curve for PCI represents Eq. 15 with $T_Q = 17$ min.

TABLE II
Purifiable Immunoprecipitable Radioactivity (PCI) as a Proportion of the Total Immunoprecipitable Radioactivity (WLI)

Minutes	Radioactivity of PCI, percentage of radioactivity of WLI			
	Single labeling		Double labeling	
	From leucine	From ALA	From leucine	From ALA
3	2.3 \pm 2.3 (3)	10.5 \pm 0.5 (2)	—	—
8	13.5 \pm 2.5 (2)	21.5 \pm 2.5 (2)	9	45
15	11.0 \pm 7.0 (2)	35.0 \pm 6.0 (2)	19	58
30	28.7 \pm 10.0 (3)	55.5 \pm 6.5 (2)	42	65
60	41.3 \pm 2.8 (3)	74.0 \pm 2.0 (2)	64	92
120	82	75.7 \pm 0.5 (2)	—	—

Values are means \pm standard error of the mean. The number of experiments is given in parentheses.

amounts were substantially higher in terms of micromoles than those used in the single-labeling experiments, especially for ALA, where the dosage was increased between 200- and 1,000-fold in the double-labeling experiments (see 10).

The leucine incorporation results fell well within the range observed in the single-labeling experiments, as can be seen in Figs. 3 and 4, where they are represented by triangles. However, close inspection of the results reveals what may possibly be a significant difference between the two sets of data. It will be noted that leucine incorporation in the double-labeling experiments tends to be high

in the TCA precipitate (Fig. 3) and low in the WLI (Fig. 4), so that the actual ratio of labeled catalase to total labeled proteins is substantially lower in the double- than in the single-labeling experiments.

The incorporation kinetics of ALA were greatly affected by the change in precursor dosage (Fig. 7). There was a marked lag in the incorporation of ALA into TCA-insoluble material, without, however, any apparent decrease of the plateau value. Incorporation of ALA into the WLI showed an even greater lag. As in the single-labeling experiments the fraction of WLI label found in the PCI

TABLE III
Long-Term Incorporation of Labeled Precursors

Precursor	Dose <i>mCi</i>	Time <i>h</i>	TCA	WLI	PCI	Percent purifiable
			precipitate			
			% dose/g liver			
$[^3\text{H}]$ Leucine	0.5	3	0.55	0.0039	0.0029	74
		18	0.38	0.0034	0.0033	97
$[^3\text{H}]$ ALA	0.25	3	1.42	0.059	0.042	71
		3	1.09	0.043	0.034	79
		18	0.59	0.072	0.071	98
		18	0.61	0.074	0.075	101

The precursors were injected intraperitoneally.

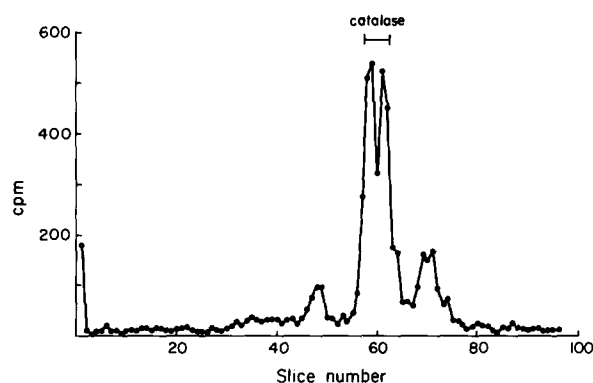


FIGURE 6 SDS-polyacrylamide gel electrophoresis of WLI isolated 8 min after injection of $[^3\text{H}]$ leucine. The sample was heated to 100°C for 5 min in the presence of 1% SDS and 0.1% β -mercaptoethanol, electrophoresed in the SDS-phosphate system of Maizel (14) on a 4% polyacrylamide gel, and stained with Coomassie blue. After staining, the gel was sliced and the radioactivity in each slice determined (13). The position and width of the stained catalase band in this gel is indicated. The nonspecific radioactivity in the immunoprecipitate (control tube) was 29% of the total, presumably accounting for the minor peaks.

was larger with ALA than with leucine as precursor (Table II).

DISCUSSION

General Features

INCORPORATION OF LEUCINE: After intraportal injection of $[^3\text{H}]$ leucine, label incorporated into TCA-precipitable material as well as into the WLI rises rapidly to a plateau which seems to remain unchanged for at least 2 h. The shape of these curves indicates that thanks to the intraportal route of injection, the specific radioactivity of the liver free leucine pool fell rapidly.

Labeled leucine enters the PCI much more slowly and progressively than it does the WLI.

The difference between the radioactivities of the two immunoprecipitates belongs to material that accompanies catalase upon immunoprecipitation, but not through purification. As label leaves this material, an equal amount becomes associated with purifiable catalase antigen. Most of this transfer takes place at a time when incorporation of labeled leucine into total protein and into the WLI has ceased. These properties clearly identify the material as playing an intermediate role in the biosynthesis of catalase. The nature of this material will be discussed below.

Essentially the same results were obtained in the single- and in the double-labeling experiments, except for a hint that in the latter experiments the synthesis of catalase may have been inhibited, or

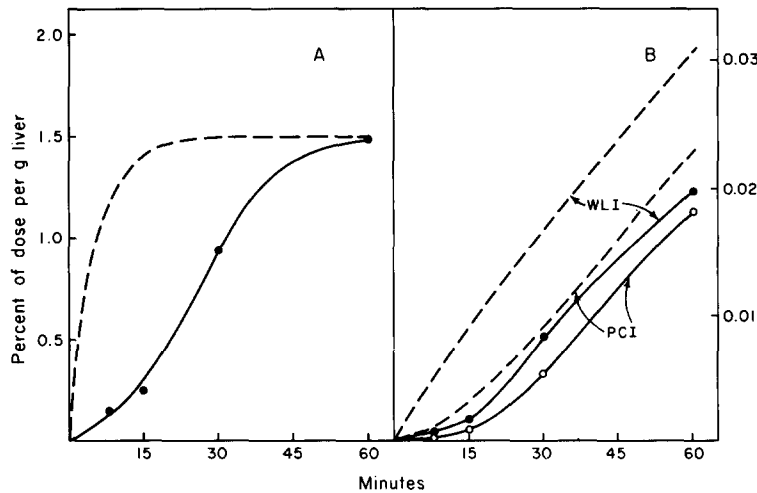


FIGURE 7 Incorporation of $[^{14}\text{C}]$ ALA (double-labeling experiments) into TCA-precipitable material (A) and into the two immunoprecipitates (B). Broken curves recall incorporation of $[^3\text{H}]$ ALA in single-labeling experiments (Figs. 3 B and 5).

that of some other protein(s) stimulated. Later in this discussion we will point out that the amounts of chemical ALA given in the double-labeling experiments were sufficient to seriously disturb the steady-state conditions of heme synthesis. Whether this disturbance affected the synthesis of catalase or of other proteins represents an interesting possibility. We did not pursue the matter further in the present investigations.

INCORPORATION OF ALA: The incorporation of $[^3\text{H}]$ ALA into TCA-insoluble material follows a course very similar to that of leucine incorporation, indicating that ALA is rapidly converted to TCA-precipitable heme or heme precursors, by way of one or more TCA-soluble intermediate pools that must all be of small size. Label entered the WLI throughout the 2 h experiment, indicating the existence between ALA and catalase-bound heme of at least one TCA-insoluble pool with a relatively long half-life and large size, most probably free heme, but possibly a reservoir of bound but rapidly exchangeable heme.

In the double-labeling experiments, where $[^3\text{H}]$ ALA was replaced by $[^{14}\text{C}]$ ALA, the incorporation kinetics were very different, being characterized by considerable lags. As will be shown more conclusively below, this difference is almost certainly due to pool inflation by the large amounts of ALA that were given in these double-labeling experiments. The resulting disturbance of the steady-state conditions may also have affected some aspect of catalase or protein synthesis, as mentioned above.

As with leucine, the PCI acquires label from ALA more slowly than does the WLI. This difference, which is seen with both $[^3\text{H}]$ ALA and $[^{14}\text{C}]$ ALA, can be similarly interpreted as indicating the existence of a heme-containing intermediate having the ability of accompanying catalase upon immunoprecipitation but not through purification.

NUMBER AND NATURE OF CATALASE BIOSYNTHETIC INTERMEDIATES: The simplest interpretation that we may consider for our results is that leucine and heme are incorporated into a single biosynthetic intermediate. If this should be the case, the kinetics of conversion of intermediate to catalase would be the same, whether the heme moiety or the polypeptide has been labeled. In fact (Table II), with the exception of a single point at 120 min, the percentage of total labeled antigen (WLI) which was converted into purifiable catalase (PCI) was always larger with ALA than with leucine as precursor. This was true in the very same rats, in the double-labeling experiments, as well as in separate groups of rats. This result might be reconciled with a single-intermediate model only if the radioactivity of the leucine pool could be shown to decay more slowly than that of the heme pool since in this case proportionately more label would continue to enter the intermediate pool from leucine than from ALA. In fact we find exactly the opposite. Therefore the single-intermediate model must be rejected. There must be at least two biosynthetic intermediates of catalase that are precipitated by anticatalase, but

do not survive purification. Both contain leucine, but only the second one contains heme. This model is illustrated in Fig. 8.

We know from the SDS-gel electrophoresis (Fig. 6) that the leucine-labeled material, which includes the two intermediates, has a monomeric molecular weight of 60,000 equal to that of catalase. Native catalase has a molecular weight of 240,000 and is believed to consist of four identical subunits (21, 22). As we will see in the following paper (10), the leucine-labeled material sediments in 0.25 M sucrose at the same rate as hemoglobin, and much more slowly than catalase itself, indicating that this labeled material is a monomer of molecular weight 60,000. Under the conditions of these experiments (8 min labeling time) approximately 89% of the label is in the first intermediate and only 9% in the second (see below, Eqs. 9 and 10). Therefore we can conclude that the first biosynthetic intermediate is an aposubunit, but we

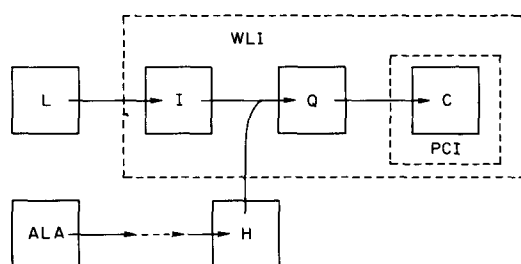


FIGURE 8 Model of catalase biosynthesis. L = leucine; I = hemeless intermediate; Q = heme-containing intermediate; C = purifiable catalase antigen; ALA = δ -aminolevulinic acid; H = heme.

cannot be sure of the molecular weight of the second. The simplest hypothesis is that it is a subunit, but other possibilities can be envisaged.

Kinetic Analysis

METHOD: The model of Fig. 8 can be represented by a well-known set of equations (see Appendix). We have attempted to fit our results to these equations, both to test the validity of the model, and, in case of a satisfactory fit, to estimate the turnover times, and thereby the pool sizes, of the biosynthetic intermediates. Fitting was done by computer by a trial and error method, using a least squares criterion of goodness of fit. The results of this analysis are summarized in Table IV.

PRECURSOR POOLS: The turnover time of the leucine pool, T_L , is estimated from the incorporation curves of leucine into total TCA-precipitable material (Fig. 3 A) and into the WLI (Fig. 4, Eq. 12). Both curves yield almost identical estimates of T_L , of the order of 2.5 min, with plateau values of $L_t = 1.2\%$ of the injected dose per gram liver for the total leucine incorporation into TCA-precipitable material, and $L_1 = 0.0055\%$ of the injected dose per gram liver for its incorporation into the WLI.

Inserting the values of T_L and L_1 , and the known rate of catalase synthesis k (about 0.12 nmol of leucine/g liver per min in our animals) into Eq. 17, we estimate the initial specific radioactivity of the free leucine pool, L_0/l , to be of the order of 0.018% of the injected dose per nanomole of leucine. From this value, in turn, we derive the leucine pool size limits given in Table IV, since we

TABLE IV
Properties of Catalase Precursor Pools

Pool	Turnover time			Size	
	Symbol	Estimate	Fig.	Symbol	Estimate
		<i>min</i>			
Leucine	T_L	2.5	3 A, 4	l	70–700†
ALA + other acid-soluble heme precursors	—	5.5	3 B	—	—
Heme	T_H	170	5	h	0.7–10‡
I intermediate	T_I	49	10	—	13§
Q intermediate	T_Q	17	9	—	4§
Catalase	—	3,100*	—	—	800§

Symbols are defined in the Appendix. Values were calculated as explained in the text.

* From references 16, 18, and 19.

† Nanomoles per gram liver.

§ Micrograms per gram liver.

know that L_o must lie between 1.2 (L_t , total incorporation into TCA precipitate) and 12.5% (quantitative uptake of the injected leucine by an 8 g liver) of the injected dose per gram liver. The resulting conclusion that rat liver must contain between 0.07 and 0.7 μmol of free leucine/g wet tissue agrees well with the values of 0.29 (4) and 0.55 (20) $\mu\text{mol/g}$ liver reported in the literature. An additional conclusion we can derive from these calculations is that the amounts of leucine injected (less than 100 nmol/g liver in all cases) did not significantly increase the size of the leucine pool (less than 1.8%).

Our estimates of the kinetic constants of the heme pool are more imprecise because the turnover time of this pool is too slow relative to the time scale of our experiments so that incorporation of [^3H]ALA into the WLI has not yet reached a plateau. As illustrated in Fig. 5, a fairly good fit with Eq. 16 is obtained with $T_H = 170$ min and $H_1 = 0.104\%$ of the injected dose per gram liver.

Less uncertainty affects the ratio H_1/T_H , which, entered into Eq. 18 together with the rate of catalase synthesis k' (about 4.4 pmol of heme/min per g liver in our animals), yields an estimate of the initial specific radioactivity of the heme pool, H_o/h , equal to 0.14% of the injected dose per nanomole of the heme. This corresponds to a maximum pool expansion of 0.025% when [^3H]ALA was given, since we injected about 11 nmol of ALA, the equivalent of 0.18 nmol of heme/g liver. With [^{14}C]ALA, however, the dosage was 200- to 1,000-fold greater, so that the total amount of ALA added was equivalent to between 5 and 25% of the heme pool. Expansion of the small preceding pools of ALA and other acid-soluble intermediates must have been much greater, and the considerable lag observed in the uptake of [^{14}C]ALA, as compared to the tritiated precursor (Fig. 7), is thereby explained.

To estimate the limits of h , the heme pool size, we have assumed that all the labeled heme, free or bound, of the liver is recovered into the TCA precipitate. Then H_o , the extrapolated initial radioactivity in the heme pool, cannot be larger than 1.5% of the dose per gram liver, the plateau value of the incorporation curve of [^3H]ALA into TCA-precipitable material (Fig. 3 B), nor smaller than 0.104% of the dose per gram liver, the estimated plateau, H_1 , of the incorporation curve of [^3H]ALA into the WLI (Fig. 5). Inserting these two limits of H_o into the estimated H_o/h ratio, we find

that h must lie between 0.7 and 10 nmol of heme/g liver (Table IV).

INCORPORATION OF ALA: The results of Fig. 5 were used to estimate T_Q , the turnover time of the heme-containing Q intermediate (Fig. 8). For this purpose the radioactivities of the PCI (C') were expressed as fractions of the radioactivities of the WLI ($Q' + C'$) and the ratio of Eqs. 15 and 16 fitted to them, using $T_H = 170$ min as estimated above. The best fit was obtained with $T_Q = 17$ min (Fig. 9). The goodness of fit of Eq. 15 to the unnormalized experimental data may be seen in Fig. 5. Since the turnover time of catalase is of the order of 3,100 min (16, 18, 19), the heme-containing intermediate represents a little more than 0.5% of the total catalase, or about 4 $\mu\text{g/g}$ liver.

INCORPORATION OF LEUCINE: The leucine results (Fig. 4) were similarly normalized and the ratio of Eqs. 11 and 12 fitted to them using $T_L = 2.5$ min and $T_Q = 17$ min (Fig. 10). The best value for T_I was 49 min, corresponding to an amount of intermediate, I, equal to 1.6% of the total hepatic catalase content, or 13 $\mu\text{g/g}$ liver. The goodness of fit of Eq. 11 to the unnormalized experimental data may be seen in Fig. 4.

The fits² are not very satisfactory, mainly because our data show little evidence of the initial lag foreseen by the theory. Such a lag is mandatory in any two-intermediate model, unless both intermediates have very short turnover times. But in the latter event the plateau would be approached much more rapidly than it is found to be. The lag is less noticeable and the fit distinctly better if only a single intermediate is assumed (broken curve in Figs. 4 and 10). But the turnover time found in this way for the leucine-labeled intermediate (70 min) is quite incompatible with the value of 17 min estimated for the ALA-labeled intermediate. The two sets of data could not be fitted to a single

² From the position of the triangles in Fig. 10, it would appear that completion of the catalase molecule occurred more rapidly in the double- than in the single-labeling experiments. Indeed, we will show in the subsequent paper that the intermediates cannot have represented more than about 1.5% of the total catalase in the double-labeling experiments (as opposed to the value of 2.1% estimated here). It is of course not at all certain that this difference is significant. It could be related to the apparent slowing down of catalase synthesis noted above as a possible effect of the injection of large amounts of ALA.

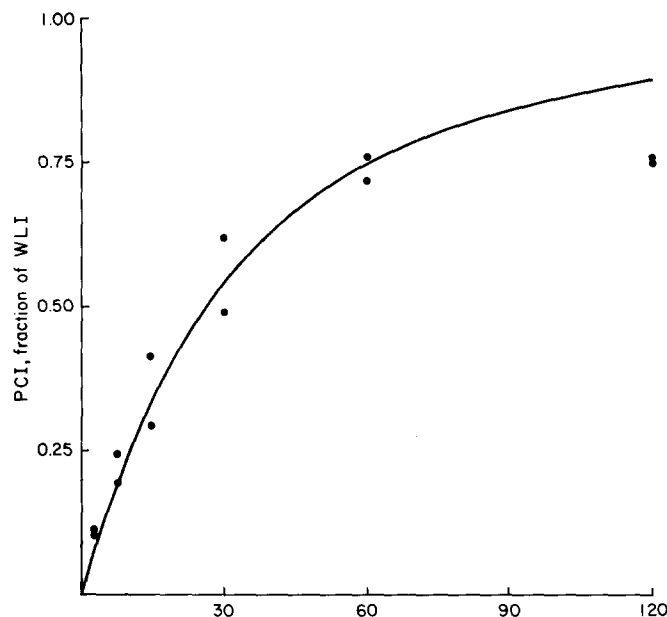


FIGURE 9 Normalized results of Fig. 5. The curve represents the ratio of Eqs. 15 and 16, with $T_H = 170$ min, and $T_Q = 17$ min.

T value, proving the fact, already stated above, that our results are not compatible with the existence of a single intermediate labeled both with leucine and with ALA.

The simplest explanation that could account for the discrepancy is that the PCIs are slightly contaminated by a radioactive impurity or that a small proportion of the intermediates survives purification. Or, it could be that the pool sizes and turnover times vary greatly in different parts of the tissue or of the cells, resulting in a composite curve depicting a combination of early and of late labeling. Alternatively, if some of the apomonomer aggregated directly to a hypothetical purifiable apotetramer, the absence of a lag would be readily understood.

CONCLUSIONS: Our interpretation of the data is summarized in Fig. 11. Catalase biosynthesis proceeds by way of at least two intermediates. The first is an aposubunit of molecular weight 60,000. It has a turnover time of 49 min and constitutes 1.6% of the total cell catalase. The second intermediate contains heme, has a turnover time of 17 min, and constitutes 0.5% of the cell catalase. The simplest hypothetical structure for it compatible with our data is that of a subunit; however, the detailed relationship between aggregation and heme addition is unknown. The fit of the theoretic

cal equations to our data is reasonably good except for the lag seen in Figs. 4 and 10. Possible reasons for this discrepancy have been discussed.

Technical Comments

The selectivity of immunoprecipitation as applied to a complex mixture like a liver homogenate, is limited by two factors: the purity of the reagents and the nonspecific precipitation that inevitably occurs. These problems are all the more serious in short-term labeling experiments such as these when a minor protein with a long half-life is precipitated; a rapidly turning over impurity can add significantly to the radioactivity of the immunoprecipitate. Catalase, whose synthesis represents only 0.45% of the total protein synthesis, is quite unfavorable in this respect.

After extensive trials, we found conditions where nonspecific precipitation was very low. The residual contamination was estimated with control serum, as explained under Materials and Methods. The following facts show that the procedures used were adequate for our purpose and free of serious artifacts: Radioactivity in the WLI reached a stable plateau (indicating the absence of rapidly turning over or secreted impurities). The radioactivities in the WLI and PCI were equal 18 h after administra-

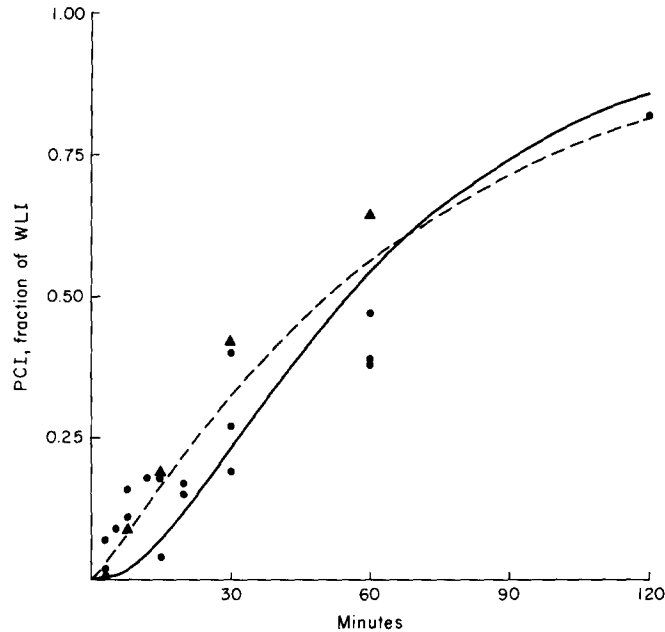


FIGURE 10 Normalized results of Fig. 4. The solid curve represents the ratio of Eqs. 11 and 12, with $T_L = 2.5$ min, $T_I = 49$ min, and $T_Q = 17$ min. The broken curve is theoretical for a single intermediate model, with $T_L = 2.5$ min and $T_Q = 70$ min.

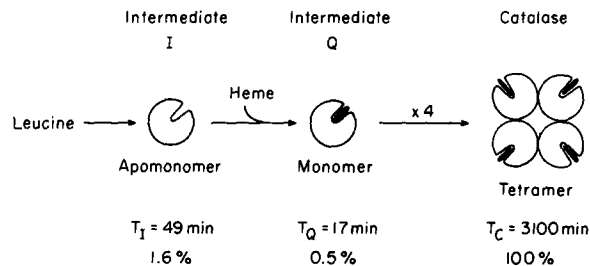


FIGURE 11 Summary of biochemical pathway of catalase synthesis. The T 's are the turnover times. The pool sizes are given as percentages of the catalase pool size. The representation of the second intermediate as a monomer is hypothetical; the detailed relationship between heme addition and aggregation is still unknown.

tion of leucine or ALA. The radioactivity of the WLI migrated on SDS-gel electrophoresis exactly as does catalase. Furthermore, as will be shown in the next paper (10), the distributions of WLI and PCI radioactivity in the liver became identical to that of catalase enzymatic activity as early as 1 h after the administration of leucine and ALA.

The authors are indebted to Brian Poole for valuable discussions and to Willenor Eaton, Fred Davidson, Armando Pelaschier, Barbara Blanchard, and Sara Gottlieb for skillful assistance.

This research was supported by grant no. GB-5796 X from the National Science Foundation.

Received for publication 17 April 1973, and in revised form 28 June 1973.

REFERENCES

1. AVRAMEAS, S., and T. TERNYNCK. 1969. The cross-linking of proteins with glutaraldehyde and its use for the preparation of immunoadsorbents. *Immunochemistry*. 6:53.
2. BAUDHUIN, P., H. BEAUFAY, Y. RAHMAN-LI, O. Z. SELLINGER, R. WATTIAUX, P. JACQUES, and C. DE DUVE. 1964. Tissue fractionation studies. 17. Intracellular distribution of monoamine oxidase, aspartate aminotransferase, alanine

- aminotransferase, D-amino acid oxidase and catalase in rat liver tissue. *Biochem. J.* **92**:179.
3. GRAHAM, R. C., JR., and M. J. KARNOVSKY. 1966. The early stages of adsorption of injected horseradish peroxidase in the proximal tubules of mouse kidney: Ultrastructural cytochemistry by a new technique. *J. Histochem. Cytochem.* **14**:291.
 4. HERBERT, J. D., R. A. COULSON, and T. HERNANDEZ. 1966. Free amino acids in the caiman and rat. *Comp. Biochem. Physiol.* **17**:583.
 5. HIGASHI, T., and H. KUDO. 1971. Specific precipitation of catalase-synthesizing ribosomes by anti-catalase antiserum. *J. Biochem. (Tokyo)*. **69**:439.
 6. KABAT, E. A., and M. M. MAYER. 1961. Experimental Immunochemistry. 2nd edition. Charles C. Thomas Publisher, Springfield, Illinois. 26.
 7. LAZAROW, P. B. 1971. Biosynthesis of peroxisomal catalase in rat liver. Proceedings of the 11th Annual Meeting of The American Society for Cell Biology. 161.
 8. LAZAROW, P. B. 1972. The biogenesis of peroxisomal catalase in rat liver. Ph.D. Thesis. The Rockefeller University, New York.
 9. LAZAROW, P. B., and C. DE DUVE. 1971. Intermediates in the biosynthesis of peroxisomal catalase in rat liver. *Biochem. Biophys. Res. Commun.* **45**:1198.
 10. LAZAROW, P. B., and C. DE DUVE. 1973. The synthesis and turnover of rat liver peroxisomes. V. Intracellular pathway of catalase synthesis. *J. Cell Biol.* **59**:507.
 11. LEIGHTON, F., B. POOLE, H. BEAUFAY, P. BAUDHUIN, J. W. COFFEY, S. FOWLER, and C. DE DUVE. 1968. The large-scale separation of peroxisomes, mitochondria, and lysosomes from the livers of rats injected with Triton WR-1339. *J. Cell Biol.* **37**:482.
 12. LEIGHTON, F., B. POOLE, P. B. LAZAROW, and C. DE DUVE. 1969. The synthesis and turnover of rat liver peroxisomes. I. Fractionation of peroxisome proteins. *J. Cell Biol.* **41**:521.
 13. LIZARDI, P. 1971. Studies on the biogenesis of mitochondrial ribosomes from *Neurospora crassa*. Ph.D. Thesis. The Rockefeller University, New York. 20.
 14. MAIZEL, J. V., JR. 1971. Polyacrylamide gel electrophoresis of viral proteins. In *Methods in Virology*. K. Maramorosch and H. Koprowski, editors. Academic Press, Inc., New York. 5:180.
 15. NOVIKOFF, A. B., and S. GOLDFISCHER. 1969. Visualization of peroxisomes (microbodies) and mitochondria with diaminobenzidine. *J. Histochem. Cytochem.* **17**:675.
 16. POOLE, B. 1971. The kinetics of disappearance of labeled leucine from the free leucine pool of rat liver and its effect on the apparent turnover of catalase and other hepatic proteins. *J. Biol. Chem.* **246**:6587.
 17. POOLE, B., T. HIGASHI, and C. DE DUVE. 1970. The synthesis and turnover of rat liver peroxisomes. III. The size distribution of peroxisomes and the incorporation of new catalase. *J. Cell Biol.* **45**:408.
 18. POOLE, B., F. LEIGHTON, and C. DE DUVE. 1969. The synthesis and turnover of rat liver peroxisomes. II. Turnover of peroxisome proteins. *J. Cell Biol.* **41**:536.
 19. PRICE, V. E., W. R. STERLING, V. A. TARANTOLA, R. W. HARTLEY, JR., and M. RECHCIGL, JR. 1962. The kinetics of catalase synthesis and destruction in vivo. *J. Biol. Chem.* **237**:3468.
 20. ROGERS, Q. R., and A. E. HARPER. 1968. Significance of tissue pools in the interpretation of changes in plasma amino acid concentrations. In *Protein Nutrition and Free Amino Acid Patterns*. J. H. Leatham, editor. Rutgers University Press, New Brunswick, New Jersey. 107.
 21. SCHROEDER, W. A., J. R. SHELTON, J. B. SHELTON, B. ROBERSON, and G. APELL. 1969. The amino acid sequence of bovine liver catalase: a preliminary report. *Arch. Biochem. Biophys.* **131**: 653.
 22. SUND, H., K. WEBER, and E. MOLBERT. 1967. Dissoziation der Rinderleber-Katalase in ihre Untereinheiten. *Eur. J. Biochem.* **1**:400.
 23. WILLIAMS, C. A., and M. W. CHASE. 1971. Photography by dark field illumination. *Methods Immunol. Immunochem.* **3**:322.

APPENDIX

Equations Used with Kinetic Analysis

The model of Fig. 8 can be represented by the following set of differential equations:

$$\frac{dL}{dt} = -\frac{L}{T_L} \quad (1)$$

$$\frac{dI}{dt} = \frac{kL}{t} - \frac{I}{T_I} \quad (2)$$

$$\frac{dQ}{dt} = \frac{I}{T_I} - \frac{Q}{T_Q} \quad (3)$$

$$\frac{dC}{dt} = \frac{Q}{T_Q} \quad (4)$$

$$\frac{dH'}{dt} = -\frac{H'}{T_H} \quad (5) \quad C = L_1 + \frac{L_1}{abc} \quad (11)$$

$$\frac{dQ'}{dt} = \frac{k'H'}{h} - \frac{Q'}{T_Q} \quad (6) \quad \cdot \left(-bT_L^2 e^{-t/T_L} + cT_I^2 e^{-t/T_I} - aT_Q^2 e^{-t/T_Q} \right) \quad (11)$$

$$\frac{dC'}{dt} = \frac{Q'}{T_Q} \quad (7) \quad I + Q + C = L_1(1 - e^{-t/T_L}) \quad (12)$$

in which, L, I, Q, C , are the total radioactivities from leucine, $H', Q',$ and C' , the total radioactivities from ALA, in the corresponding pools (per gram liver); the T 's are the turnover times of the pools³; k and k' are the rates of synthesis of catalase in nanomoles per minute per gram liver, of leucine and heme, respectively; l and h are the respective pool sizes of leucine and heme in nanomoles per gram liver.

Two simplifications have been introduced in these equations: the decay of catalase, which is less than 4% in 2 h, has been neglected in Eqs. 4 and 7; participation of ALA and of the intermediates between ALA and heme has been neglected in Eq. 5. By heme pool is meant the pool from which label administered as ALA enters the Q intermediate.

The solutions to this set of differential equations are the following:

$$L = L_0 e^{-t/T_L} \quad (8)$$

$$I = \frac{L_1 T_I}{a} \left(e^{-t/T_L} - e^{-t/T_I} \right) \quad (9)$$

$$Q = \frac{L_1 T_Q}{abc} \cdot \left(bT_L e^{-t/T_L} - cT_I e^{-t/T_I} + aT_Q e^{-t/T_Q} \right) \quad (10)$$

³ The turnover time is related to the corresponding half-life, $t_{1/2}$, by $t_{1/2} = 0.693 T$.

$$H' = H_0 e^{-t/T_H} \quad (13)$$

$$Q' = \frac{H_1 T_Q}{T_H - T_Q} \left(e^{-t/T_H} - e^{-t/T_Q} \right) \quad (14)$$

$$C' = H_1 + \frac{H_1}{T_Q - T_H} (T_H e^{-t/T_H} - T_Q e^{-t/T_Q}) \quad (15)$$

$$Q' + C' = H_1(1 - e^{-t/T_H}) \quad (16)$$

L_0 and H_0 are constants of integration and equal the extrapolated initial total radioactivities in the leucine and heme pools, respectively. $a, b,$ and c equal $T_L - T_I, T_I - T_Q,$ and $T_L - T_Q,$ respectively. L_1 and H_1 are also defined in terms of previous constants:

$$L_1 = kL_0 T_L / l \quad (17)$$

$$H_1 = k'H_0 T_H / h \quad (18)$$

Inspection of Eqs. 12 and 16 indicates that L_1 and H_1 are the total leucine and heme radioactivities that will ultimately be incorporated into catalase. Operationally, C and C' are the radioactivities in the PCI, whereas $I + Q + C$ and $Q' + C'$ are the radioactivities in the WLI.